

A Nested Marker for Augmented Reality

Keisuke TATENO, Itaru KITAHARA, and Yuichi OHTA

Graduate School of Systems and Information Engineering, University of Tsukuba

ABSTRACT

A Nested Marker, a novel visual marker for camera calibration in Augmented Reality (AR), enables accurate calibration even when the observer is moving very close to or far away from the marker. Our proposed Nested Marker has a recursive layered structure. One marker at an upper layer contains four smaller markers at the lower layer. Smaller markers can also have lower-layer markers nesting inside them. Each marker can be identified by its inside pattern, so the system can select a proper calibration parameter set for the marker. When the observer views the marker close-up, the lowest layer marker will work. When the observer views the marker from a distance, the top-layer marker will work. It is also possible to simultaneously utilize all visible markers in different layers for more stable calibration. Note that Nested Marker can be used in a standard ARToolkit framework. We have also developed an AR system to demonstrate the ability of Nested Marker.

1 INTRODUCTION

Augmented Reality is a technology that merges virtual objects with the real world. The accuracy of geometric registration between real and virtual spaces critically influences the reality felt by users in augmented reality systems. Therefore, geometric registration is one problem in augmented reality.

In recent years, vision-based registration methods with visual markers (e.g., ARToolkit [1], CyberCode [2], ArLoc [3], ARStudio [4], ARTag [5]) have become actively used with the improvements of the processing performance of computers. Since a virtual object is superimposed based on the position of the captured visual marker placed in a real space, it is possible to realize highly accurate geometric registration. Moreover, since vision-based methods do not need any special sensors except a capturing camera, realizing an AR system is quite easy.

Since the accuracy of geometric registration depends on the appearance of a captured marker, the size and layout of the marker must be carefully considered. When the positional relationship between camera and marker changes, however, the captured appearance also changes. Thus, even in vision-based methods, there is a limitation problem: viewpoint movement.

This paper proposes Nested Marker that expands the range of viewpoint movement by employing hierarchically structured markers with various sizes. By choosing a marker with an appropriate size for observing distance, we can realize accurate geometric registration that enables larger viewpoint movement from a close-up to a long distance view.

2 RELATED WORKS

The ARToolkit is a widely used application library to realize Augmented Reality systems. Square-shaped ARToolkit markers are used to calculate camera pose and identify their Identification

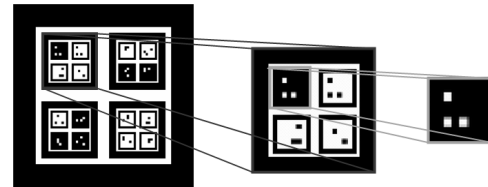


Figure 1. Nested Marker

Data (IDs). The relative pose between the capturing camera and marker are estimated by the appearance of the captured marker. Many AR systems use multiple markers combining two or more markers to realize robust geometric registration to partial occlusions of the marker and achieve a wider observation area [6]. However, installing such multiple markers everywhere in real space is unreasonable because they are too conspicuous. Moreover, multiple marker schemes still have a limitation: observing distance depends on the size of individual markers. If multiple markers are comprised of small markers, it is possible to realize geometric close-up registration. However, when the markers are observed from a long distance, the resolution of the captured marker remarkably decreases. As a result, it is difficult to realize accurate geometric registration from a distance. Nested Marker is a novel and an improved version of the ARToolkit marker to solve the above problems. Our Nested Marker is designed within the standard framework of the ARToolkit to fully utilize its great implementation.

3 PROPOSED METHOD

In this section, we introduce our proposed visual marker that can realize accurate geometric registration when observation distance drastically changes.

3.1 Nested Marker

As shown in Figure 1, Nested Marker has a recursive layered structure. There is a marker in the upper layer and four smaller markers in the lower layer. Smaller markers also have lower-layer markers nesting inside them. Every marker at every layer is designed to be identified by its interior pattern, which is composed of lower-layer markers. The largest marker visible from the camera is dynamically selected based on the distance between observer and marker. When the observer watches the marker at close range, the lowest layer marker is used for geometric registration. When the observer watches the marker from a distance, the top-layer marker is used. Since each marker can be identified by its interior pattern, the system selects the appropriate calibration parameter set for the marker. It is also possible to simultaneously utilize all the visible markers in different layers for more stable calibration. So even if a captured marker is partially occluded by other objects, the correct camera parameter can be estimated by our Nested Marker and choosing an appropriate non-occluded marker in the captured image.

1-1-1 Tennoudai, Tsukuba, Ibaraki, 305-8573, Japan
Email: {taten, kitahara, ohta}@image.iit.tsukuba.ac.jp

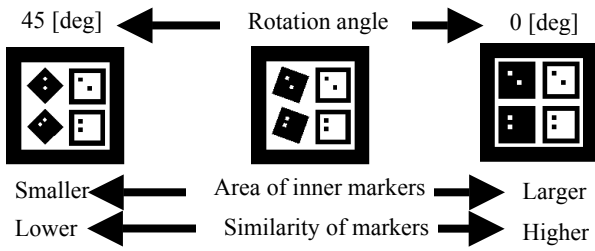


Figure 2. Rotation angle of inner markers

3.2 Design policy of Nested Marker

By choosing a marker with an appropriate size for each observing distance, stable and accurate geometric registration can be achieved that enables huge movement of viewing position. Therefore, we have to carefully consider the moment of switching a marker chosen for registration. The accuracy of geometric registration depends on the captured size of markers. When the captured size of the marker is large, estimated pose parameters are more accurate. If the area of the lower-layer marker is much smaller than the upper-layer marker, the accuracy of pose parameters estimated from those markers changes considerably while switching between the two layers. Such large discontinuity causes discomfort for observers of the AR scene. Therefore, when designing Nested Marker, the size of the lower-layer markers must be enlarged as much as possible.

Three parameters must be considered in Nested Marker design: rotation angle between lower- and upper-layer markers, number of lower-layer markers at each layer, and thickness of the marker frame. We will explain how to set each parameter.

3.2.1 Rotation angle between markers

Figure 2 shows the relationship of similarity between markers and their area when the rotation angle of the inner markers is changed. If the rotation angle of every inner marker is fixed to 0° , the area of the lower-layer inner marker becomes the largest. However, since the rotation angle of the lower-layer markers is identical to the upper layer marker, the maximum similarity value among markers in the two layers may become the largest. On the other hand, as shown on the left of Figure 2, if the rotation angle of each lower-layer marker is different, similarity values among markers may decrease because each upper-layer marker contains inner markers with different rotation angles. However, in this case, the area of inner markers becomes smaller because a margin around each inner marker is necessary to rotate the marker pattern. As described above, we give higher priority to the marker area and therefore fix the rotation angle of inner markers to 0° .

3.2.2 Number of inner markers at each layer

The total number of markers in a Nested Marker depends on the number of inner markers at each layer and the depth of hierarchy. Figure 3 shows examples where the number of inner markers at each layer is 1, 4, and 9. The bigger the increase of inner markers, the more robust to partial occlusion the Nested Marker will become. However, as the number increases, the area of the inner markers becomes smaller compared to the upper-layer marker. This difference of marker size causes a difference of estimation accuracy during switching between marker layers. Moreover, when the number of markers increases, it becomes difficult to maintain maximum similarity among markers at a reasonably lower value. On the other hand, if the number of inner markers at each layer is too few, observable space with a close-up view becomes narrower because the positions of the inner markers are

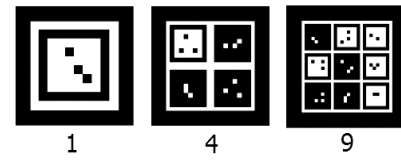


Figure 3. Number of lower-layer makers at each layer

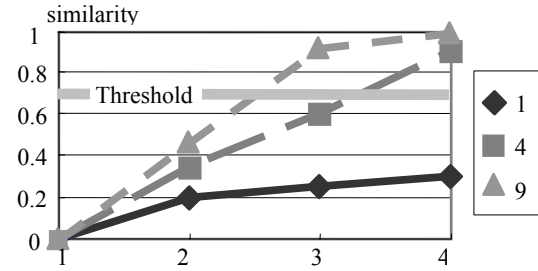


Figure 4. Maximum similarity between markers

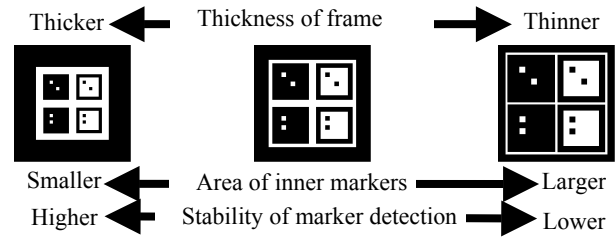


Figure 5. Thickness of marker frame

biased inside the upper-layer marker.

Figure 4 shows the relation between the maximum similarity value among markers and the number of inner markers at each layer and the depth of hierarchy. The maximum similarity value approaches 1.0 as the number of inner markers and the depth of hierarchy increase. If the maximum similarity value is too large, marker identification easily fails. We chose a threshold of 0.7 as a similarity value to prevent the marker identification process from easily failing in practical use. As a result, the number of inner markers is set to 4, and the depth of hierarchy is set to 3.

3.2.3 Thickness of marker frame

Figure 5 shows the relationships of the area of inner markers and the stability of marker detection with the thickness of the marker frame. The thickness of marker frame is critical for the stability of marker detection. In AR systems, since the camera is often mounted on users' heads, motion blur frequently occurs, which is caused by rotation and translation of the head. When the marker frame is thick, the motion blur of the marker frame does not seriously damage the marker detection process. Therefore, even when the head moves rapidly, stable marker detection is possible. On the other hand, as shown in Figure 5, when the marker frame is thick, the inner marker area becomes small. We chose a minimum thickness of marker frame to satisfy the following requirement. For simplicity, we approximate motion blur as translation on the image caused by head rotation. Based on this assumption, we calculate the appropriate thickness of marker frame as follows. Blur width B by motion blur can be represented as Eq. 1. Here, ω is the angular speed of the rotational movement of a capturing camera, d is the distance from the camera to the captured marker, and t is the shutter speed of the camera. When blur width B is less than thickness F of the marker frame, stable marker detection is possible:

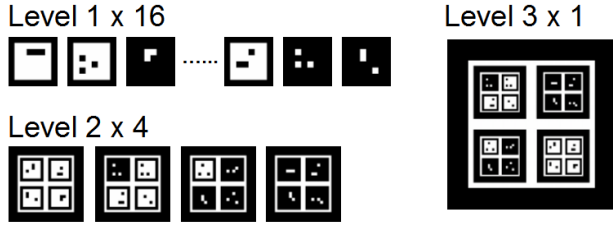


Figure 6. Results of the assembling algorithm

$$2d\pi \frac{\omega t}{2\pi} \approx B < F \quad (\text{Eq.1})$$

We calculate blur width by assigning a parameter of observation action in an ordinary AR scene to Eq. 1. As the angular speed of head rotation, we must know the speed of typical head rotation when observing an object. We set angular speed to 30 deg/sec because that is the maximum speed of Smooth Pursuit Eye Movement [7], which is the smooth movement of eyes when following a moving object. An appropriate distance from the marker to the camera depends on marker size. For example, when assuming an AR scene in which a marker with an 80 mm square area is put at a distance where the hands are reachable (i.e., d is set to 500 mm) and the shutter speed of capturing camera t is 1/30 sec, the width of motion blur becomes 8.72 mm.

3.3 Assembly scheme of Nested Marker

For Nested Marker, the ID pattern of the upper-layer marker is composed of lower-layer markers, and every marker at every layer must be identified by its inside pattern. We have developed an automatically assembling Nested Marker scheme.

The lowest layer marker of Nested Marker is expressed by a 2D pattern of 16 black and white dots that are set in a 4 x 4 reticular pattern. Two types of 2D patterns are distinguished by background color: black or white. Three dots in 16 are used to prevent the area ratio of ground and code colors from being reversed. As a result, $560 \times 2 = 1120$ patterns can be used to express a pattern of the lowest layer marker. The lower-layer marker can be used as the ID pattern of the upper-layer marker by biasing the distribution of the background color of the lower-layer marker.

First, we decide the number of markers at the uppermost layer. Then the number of markers that comprises Nested Markers in each layer is calculated. The number of markers n_h at hierarchical level h can be obtained by the recurrence formula: $n_{h-1} = n_h \times 4$.

Next, we decide the pattern of the level 1 marker, which is the lowest layer marker. It is composed of two white and black backgrounds and 560 dot patterns. When n_1 kinds of dot patterns are necessary to compose Nested Marker, we choose n_1 patterns from 560 patterns with a fixed background color; the number of all combinations M is obtained as ${}_{560}C_{n_1} = M$.

These M sets of n_1 dot patterns are the candidates of the lowest layer markers. Similarity is calculated between every pair of patterns in each set, and maximum similarity in the set is obtained. We select a set of dot patterns whose maximum similarity is the lowest in all sets of dot patterns. Two kinds of selected sets of dot patterns with different background colors comprise the ID pattern of the lowest layer markers.

Next, the pattern of upper-layer markers is decided. The level h marker is composed of four level $h-1$ markers. When n_h kinds of level h markers are composed by choosing the sets of four

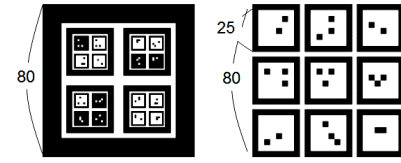


Figure 7. Experimental objects

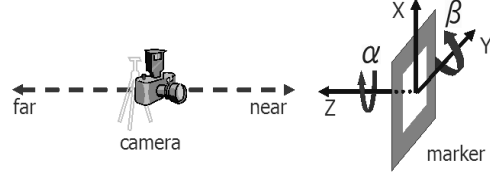


Figure 8. Spatial relationships in the experiment

markers from n_{h-1} level $h-1$ markers, the number of all combinations M is obtained from Eq. 2:

$$\sum_i^{n_h} ({}_{n_{h-1}-4i}C_4) = M \quad (\text{Eq.2})$$

These M sets of n_h markers are candidates of level h markers. Similarity is calculated between every pair of level h markers in each set and the lower layer markers that were already determined, and maximum similarity in the set is obtained. We select the set of level h markers whose maximum similarity is the lowest in all the M candidates of level h markers.

Next, the same process is repeated until the uppermost layer marker is produced. Figure 6 shows an example of Nested Marker assembled by this algorithm.

4 EVALUATION OF ACCURACY FOR POSE ESTIMATION

In this section, we introduce evaluation experiments of the accuracy of geometric registration using Nested Markers.

When conducting evaluations using images of real space, we must consider such noise factors as lighting conditions and the radial distortion of the camera lens. Then, we conducted a simulation experiment using artificially rendered images to evaluate the innate ability of Nested Marker to calculate geometric registration. The marker's rendering image is a binary image that does not contain lighting effects or radial distortion. In the experiment we used a Nested Marker with three layers, as shown on the left of Figure 7. For comparison with ordinary ARToolkit markers, we used a set of multiple markers consisting of nine markers shown on the right of Figure 7. The size of the uppermost layer of both markers is set to 80 mm square. Figure 8 shows the spatial relationship between the markers and the virtual camera. The slant of the marker plane against the virtual camera is fixed to 30°. The distance between the marker and the virtual camera changes from 30 to 800 mm at 10 mm intervals. The six pose parameters as 3D positions (X, Y, Z) and 3D rotation angles (alpha, beta, gamma) are estimated by processing the marker images. The error of the true and estimation values is used to evaluate the accuracy of pose estimation.

Figure 9 shows the error results on Z and alpha. The position and orientation errors are most remarkable on Z and alpha, respectively. The vertical axis is estimation error, and the horizontal axis is the distance between markers and camera. The black line shows the result by Nested Marker, and the gray dot line shows the result by multiple markers. As shown on the left of Figure 9, when the distance was larger than 480 mm, serious and irregular estimation errors frequently occur on Z by multiple markers. On the other hand, estimation error by Nested Marker is

stable and increases with distance. As shown on the right of Figure 9, when the distance was larger than 480 mm, serious and irregular estimation errors frequently occurred on slant angle alpha by multiple markers. On the other hand, estimation error by Nested Marker was stable. In AR applications, when estimation error drastically changes in successive frames, the superimposed CG jitters in the video sequence, which are uncomfortable to watch. From these results, we confirm that Nested Marker outperforms multiple markers for AR applications with large zoom in and out camera motions.

5 APPLICATIONS USING NESTED MARKER

Compared with an ordinary visual marker, geometric registration with Nested Marker has the following two positive features. One is the range of user view movement that enables close-up to the marker. The other is robustness to partial occlusion of the marker. Therefore, zooming in on a virtual object and observing the details, which is difficult in ordinary AR applications, can be achieved using our Nested Marker. Next, a 3D model viewer with Level of Detail was constructed as an AR application example that fully utilizes the Nested Marker characteristics. For the experiment, we used a note PC (CPU: Pentium M 1.6 GHz, Memory: 1.0 GByte, Graphics card: Intel Graphics media accelerator 900) and a USB camera (Logitech Qcam for Notebooks Pro, resolution: 640 x 480 pixels, frame rate: 30 fps). In this system, we generated a Nested Marker of three layers. The size of the level 3 layer marker (uppermost layer) is 80 mm, the size of the level 2 layer marker is 25 mm, and the size of the level 1 layer marker is 8 mm.

The results of the AR scene with Level of Detail, when the camera is moved within a range from 800 to 40 mm, are shown in Figure 10. The distance between the marker and the camera is 800 mm at the upper left, 400 mm at the upper right, 40 mm at the lower left, and 21 mm at the lower right. When a camera is watching a 3D virtual object at a distant position, the object is represented by a simple 3D model. When the camera zooms in on the model, the model is represented by a detailed 3D model. By using Nested Marker, observing a virtual object from overview to details is possible, regardless of the change in distance. The results show the largeness of the range of user view movements.

6 CONCLUSION

As proposed in this paper, Nested Marker is a hierarchically structured visual marker that enables a close-up view of an AR scene and effectively enlarges the visual range of observers. Nested Marker can be easily installed on commercial devices such as PCs and USB cameras because it is designed in the standard framework of ARToolkit. To realize accurate geometric

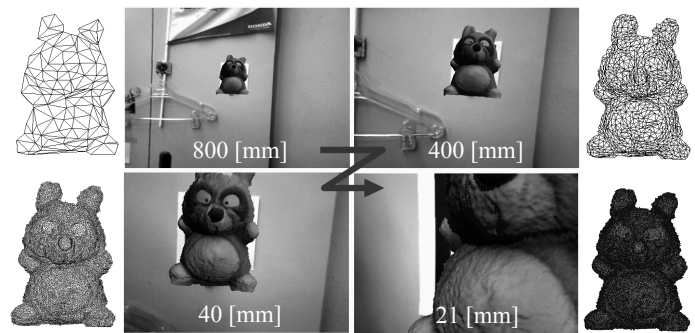


Figure 10. AR scene when camera is moving

registration at various distances, we carefully considered the design policy of Nested Marker and determined the parameters that define its appearance. We described an assembly scheme of Nested Markers. Evaluation experiments using artificially rendered marker images illustrate its ability with comparisons to ordinary markers in both the width of visual range and stability of pose estimation. We also developed an AR application to demonstrate the ability of Nested Marker. In the future, we will evaluate the accuracy of marker identification when blur and noise under a real environment are contained in the marker image.

REFERENCES

- [1] H. Kato and M. Billinghurst, "Marker Tracking and HMD Calibration for a video-based Augmented Reality Conferencing System," In Proceedings of the 2nd International Workshop on Augmented Reality (IWAR 99). October, San Francisco, USA, 1999.
- [2] J. Rekimoto and Y. Ayatsuka, "CyberCode: Designing augmented reality environments with visual tags," Proc. Designing Augmented Reality Environments (DARE) 2000, Apr. 2000.
- [3] X. Zhang and N. Navab, "Tracking and pose estimation for computer assisted localization in industrial environments," In IEEE Workshop on Application of Computer Vision, pp. 214-221, 2000.
- [4] S. Malik, G. Roth, and C. McDonald, "Robust 2D Tracking for Real-Time Augmented Reality," Proceedings of Vision Interface (VI) 2002, Calgary, Alberta, Canada. pp. 399-406, 2002.
- [5] M. Fiala, "ARTag Revision 1, A Fiducial Marker System Using Digital Techniques," NRC/ERB-1117. November 24, 2004.
- [6] E. J. Umlauf, H. Piringer, G. Reitmayr, and D. Schmalstieg, "ARLib: the augmented library," Proc. Int'l Workshop on ARToolkit, 2002.
- [7] S. Mishima, "Dictionary of Eyes (in Japanese)," pp.200, Asakurashoten, 2003.

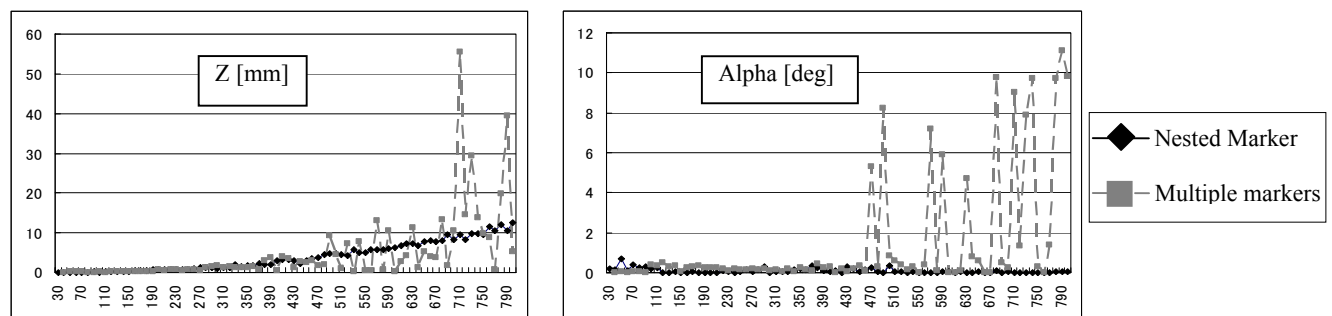


Figure 9. Results of experiment